Thermal Effects and Band Spreading in Capillary Electro-Separation

J. H. Knox

Wolfson Liquid Chromatography Unit, Department of Chemistry, University of Edinburgh, West Mains Road, Edinburgh EH9 3JJ, UK

Key Words

Capillary Electroseparation Methods (CES)
(Capillary) Electrophoresis
(Capillary) Electrochromatography
Thermal effects (in CES)
Band spreading (in CES)
Optimisation (of CES)

Summary

Four Capillary Electroseparation methods are distinguished. All have an ultimate efficiency limited only by axial diffusion and are in principle capable of achieving 10^6 plates in < 1 hour.

The main limitation to performance arises from Ohmic heating of the electrolyte. While forced convection at $10\,m\,s^{-1}$ is recommended to keep tubes cool, the parabolic temperature profile within the electrolyte limits the tube bore which can be used. A simple limiting expression is derived: $(d_c/\mu m)^3\,(E/kV\,m^{-1})^3\,(c/mol\,dm^{-3}) < 3.3 \times 10^9$.

Introduction

Four distinct capillary electroseparation methods have been described to date:

(A)	Capillary zone electrophoresis	CZE	[1–6]
(B)	Capillary gel electrophoresis	CGE	[7, 8]
(C)	Capillary micellar electrokinetic chromatography	CMEC	[9–13]
(D)	Capillary electroendosmotic chromatography	CEC	[14–16]

These four techniques can all be carried out in the equipment outlined diagrammatically on Fig. 1. Columns are 200–1000 mm long and up to 200 μm in bore, and in the configuration shown may be straight rigid tubes. The voltage applied can be up to 50 kV. Beyond this problems arise from electrical breakdown of the air and corona discharge, but there is no ultimate restriction if these problems can be solved. The high voltage end of the system must be enclosed in a Faraday cage with appropriate safety locks. Injection is achieved by filling the injector/reservoir with analyte solution, applying a small potential or suction for a few seconds, washing the injector/reservoir thoroughly with eluent and finally applying the operating potential. Detection is normally in-column using either a fluorescence or UV monitor. In the latter case high sensitivity and stability are required, and a noise level of $< 10^{-5}$ AU is desirable since the path length is equal to the tube bore.

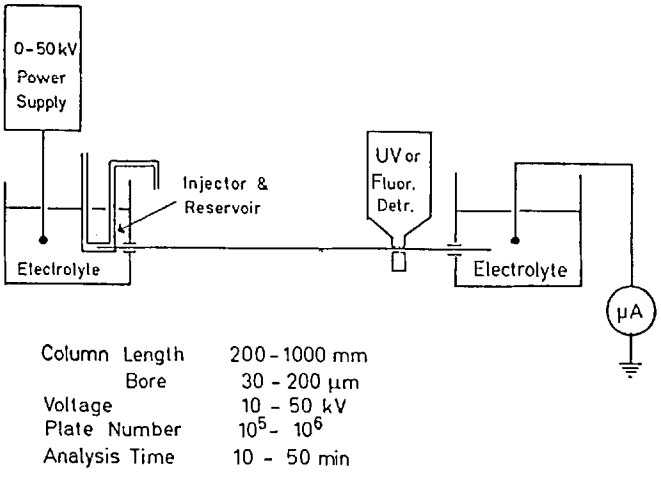

Fig. 1
Outline of equipment for Capillary Electro-Separations.

The four methods variously use open tubes or tubes containing gels or particles. They can separate ionized or neutral solutes. Their main characteristics are summarized in Table I.

Migration Mechanism

Migration of solutes within a CES system arises from one or both of the following phenomena:

A. Electrophoresis

Ionized solutes in an electric field move within bulk electrolyte at velocities which depend upon their charge and size.

0009-5893/88 0329-09 $ 03.00/0

Table I. Characteristics of capillary electroseparation methods.

Method	Phases		Solute Type	Basis of Separation	Factors Limiting Performance
	Electrolyte	Alternate			
1. CZE	M	n.p.	I	E	T, D
2. CGE	S	S	I	OE	T, D
3. CMEC	M	M	N, IP	P	T, D
4. CEC	M	S	N, IP	P	T, D, MT

Phases: M = moving, S = stationary
Solute Type: I = ionized, N = neutral, IP = ion pair
Basis of Sepn: E = electrophoresis, OE = obstructed electrophoresis, P = partition between phases
Factors Limiting Performance: T = thermal effects, D = axial diffusion, MT = slow mass transfer

Any charged particle in an electrolyte is part of an electrical double layer system where the fixed charge of the particle itself is neutralized by oppositely charged ions, some of which are more or less irreversibly attached to the particle and some of which are free to diffuse within the bulk electrolyte and exchange with ions in the bulk electrolyte. In an electric field, shearing occurs at the interface between the fixed ions and the free ions. The electrical potential at this interface is called the zeta potential (denoted by ζ).

The electrophoretic velocity of any particle in such a situation is given by

$$u_{ep} = \frac{2}{3}\frac{\epsilon_0 \epsilon_r \zeta E}{\eta} \quad (1)$$

A full discussion of the Stern Gouy Chapman theory of the electrical double layer is given in standard textbooks [17]. Typically the zeta potential is in the range 0 to 50 mV. Thus with $E = 50\,kV\,m^{-1}$, $\zeta = 50\,mV$, $\eta = 0.001$, $kg\,m^{-1}\,s^{-1}$ and $\epsilon_r = 80$ we obtain $u_{ep} = 1\,mm\,s^{-1}$.

B. Electroendosmosis

Since all surfaces are in principle charged, an electrical double-layer exists at any surface in contact with an electrolyte. When a field is applied parallel to the surface, as is done in CES systems, the liquid will move under the field according to an equation very similar to (1) namely —

$$u_{eo} = \frac{\epsilon_0 \epsilon_r \zeta E}{\eta} \quad (2)$$

The 2/3 factor, present for movement of a spherical particle, is unity for a cylindrical unit such as the liquid in a capillary. Eqs. (1) and (2) apply when the thickness of the double layer δ is much less than the extent of the electrolyte beyond the double-layer. In the case of electroendosmosis it is shown by Rice and Whitehead [19] as discussed previously by Knox and Grant [20] that the channel diameter, d_c, must be at least 10δ if double-layer overlap is not to cause a loss of electroendosmotic velocity. The double-layer thickness is given by

$$\delta = \left\{\frac{\epsilon_0 \epsilon_r RT}{2cF}\right\}^{1/2} \quad (3)$$

For $c = 10^{-3}\,mol\,dm^{-3}$ in water $\delta = 10nm$. While double-layer overlap is no problem in the CES methods which use open tubes, it is important with packed tubes where the smallest possible particles should be used. Since the channels in beds of spheres are approximately 1/4 of the mean sphere diameter, the particle diameter below which significant loss of electroendosmotic velocity will occur is expected to be about 40δ, that is about $0.4\mu m$ for 10^{-3}M solutes. Table II indicates the values of δ and minimum d_p for other concentrations of aqueous electrolyte. The general validity of this was confirmed by Knox and Grant who demonstrated that there is indeed no significant loss of electroendosmotic velocity with particles down to $1.5\mu m$ in diameter [16].

Table II. Double layer thickness, δ, and minimum particle diameter, d_p, for full electroendosmotic flow rate.

$c/mol\,dm^{-3}$	0.001	0.01	0.1
δ/nm	10	3	1.0
$d_{p(min)}/\mu m$	0.4	0.12	0.04

Separation Mechanisms

The mechanisms by which solutes separate in the four techniques are illustrated diagrammatically on Fig. 2.

In CZE the bulk electrolyte in the tube migrates under electroendosmosis while the solute ions move within the bulk at their individual electrophoretic velocities. Each solute ion then moves down the tube at a rate given by

$$u_x = u_{eo} + u_{ep} \quad (4)$$

where u_{ep} can have the same or opposite sign to u_{eo}. Separation of solutes depends upon different values of their electrophoretic velocities or mobilities. (The electrophoretic mobility is $\mu_{ep} = u_{ep}/E$).

In CGE the strands of the gel constrict the passages through the column and, being much closer together than the electrical double-layer thickness, δ, they prevent any electroendosmotic flow. In addition the composition of electrolyte is specifically chosen to minimize the zeta potential. Separation thus depends upon obstructed electrophoresis. In the absence of the gel, large nucleotides, for example, tend to migrate at similar speeds irrespective of size since

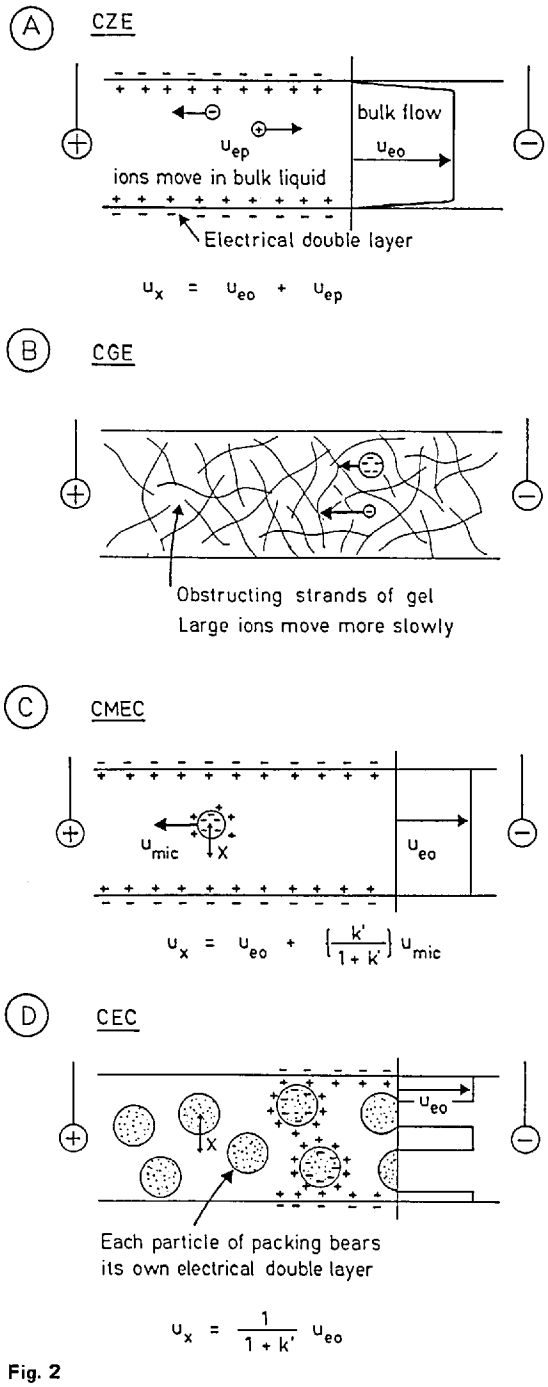

Fig. 2

Diagramatic representation of

A) Capillary zone electrophoresis, CZE

B) Capillary gel electrophoresis, CGE

C) Capillary micellar electro-kinetic chromatography, CMEC

D) Capillary electro-chromatography, CEC

u_x is the linear migration velocity of the analyte X. u_{eo} = electro-endosmotic velocity; u_{ep} = electrophoretic velocity; k' = phase capacity ratio.

they all possess similar zeta potentials — as do micellar and colloidal particles of different sizes. However, in CGE, they can be separated on the basis of their size. The obstructed electrophoretic velocity can be given as

$$u_{oep} = \frac{2}{3} \frac{\epsilon_0 \epsilon_r \zeta E}{\eta} \times \chi \qquad (5)$$

where χ is a geometrical obstructive factor, less than unity, which decreases as the solute size increases.

In CMEC unionized solutes are partitioned between bulk electrolyte moving at the electroendosmotic velocity u_{eo} and an alternate phase, the micelles, which move within the bulk electrolyte at a velocity u_{mic}. If k' is the capacity ratio given by eq. (6)

$$k' = \frac{\text{quantity of solute in micellar phase}}{\text{quantity of solute in bulk electrolyte}} \qquad (6)$$

then the migration velocity of any solute is readily shown to be

$$u_x = u_{eo} + \left(\frac{k'}{1+k'}\right) u_{mic} \qquad (7)$$

This equation is equivalent to those of Terabe et al. [9] and of Cohen et al. [12]. Here u_{mic} may have the same or (preferably) opposite sign to u_{eo}. In general since $u_{mic} < u_{eo}$ solutes will always migrate in the direction of the bulk liquid even if the signs of u_{mic} and u_{eo} are opposite.

In CEC the column is packed with an adsorbent, for example a typical HPLC packing material The alternate phase is now stationary, as in normal chromatography, and the migration velocity of any solute is given by —

$$u_x = \frac{1}{1+k''} u_{eo} \qquad (8)$$

where

$$k'' = \frac{\text{quantity of solute in mobile zone (outside particles)}}{\text{quantity of solute in stationary zone (inside particles)}} \qquad (9)$$

It may be noted that if u_{mic} in eq. (7) is replaced by $-u_{eo}$, to give a stationary alternate phase, eq. (8) results.

Ultimate Performance — Plate Height

Jorgenson [1] showed that with a plug flow profile in an open tube, the plate efficiency in CZE would ultimately be limited only by axial diffusion. Accordingly the lowest possible HETP in CZE is

$$H = \frac{2D_m}{u} \qquad (10)$$

Since u, the linear velocity of the solutes approximates to u_{eo}, H is given by

$$H = \frac{2D_m \eta}{\epsilon_0 \epsilon_r \zeta E} \qquad (11)$$

For typical values (see glossary) H = 1.1 μm. We may thus expect up to 900,000 plates per metre with E = 50 kV m^{-1}.

The technique of CGE will have the same limitation but here solute migration occurs entirely by obstructed electrophoresis. Thus —

$$H = \frac{2D_m}{\epsilon_0 \epsilon_r \zeta E \chi} \qquad (12)$$

As molecular diameter increases both D_m and χ will fall thus H may be expected to remain more or less constant

and have a value similar to that in CZE for a molecule of the same size. Such efficiencies have been demonstrated by Cohen et al. [7, 8].

In CMEC once again axial diffusion is the ultimate limitation and eq. (10) applies. The micelles are so small that there is no mass transfer limitation. Once again such efficiencies have been repeatedly demonstrated [9–13].

For CEC the situation is strikingly different. Here, as in pressure driven HPLC, the plate height is determined not only by axial diffusion but by flow dispersion and resistance to mass transfer. The complete Van Deemter equation (or equivalent) must be used, for example,

$$H = 2\lambda d_p + \frac{2\gamma D_m}{u} + \frac{1}{30}\frac{k''}{(1+k'')^2}\frac{d_p^2 u}{D_{sz}} \qquad (13)$$
$$= A + B/u + Cu$$

The A-term represents the contribution from flow inhomogeneity in the packed bed, that is from stream splitting and velocity variation within and between channels. Fig. 3 shows how the axial flow rate might be expected to vary within a packed bed under electroendosmotic and pressure flow conditions. In the latter there will be a parabolic flow distribution over any channel (taken as cylindrical for simplicity) and the mean flow rate, $\bar{u}$, will vary from channel to channel being greatest in the widest channels. Under electroendosmotic flow all velocities will be almost identical since u_{eo} does not depend upon channel diameter at least when $d_c > 10\delta$. This leaves only the contribution from the variability in the direction of flow as the liquid negotiates the various obstacles in its flow presented by the particles.

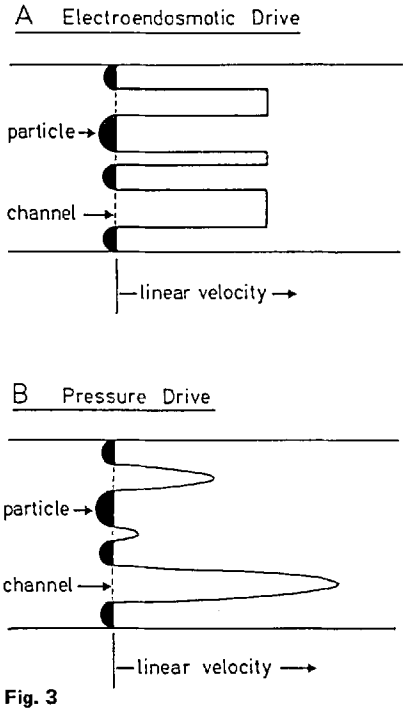

Fig. 3

Showing different idealized flow profiles in a packed bed (the shaded semicircles represent the particle of the bed) under (A) electrical and (B) pressure drive.

Thus in CEC we expect the A-term to be much less than in HPLC for any particular particle size, d_p. A can, of course, be reduced by reducing d_p. This has been demonstrated by Knox and Grant [16].

The C-term in eq. (13) arises from the non-instantaneous rate of equilibration of solute between the particles and the liquid flowing outside them. The key parameter is the effective diffusion rate of solutes within the particles D_{sz} which has been discussed by Knox and Scott [18] and is given by –

$$D_{sz} = D_m \frac{\gamma_{sm}\phi + [k''(1-\phi) - \phi]\gamma_s (D_s/D_m)}{k''(1-\phi)} \qquad (14)$$

where γ_{sm} and γ_s are the obstructive factors for diffusion in the stagnant mobile phase and stationary phase respectively, and where ϕ is the proportion of mobile phase within the particles.

Under conditions where the diffusion rate within the stationary phase, D_s, is very slow, D_s/D_m becomes negligible and –

$$D_{sz} = D_m \frac{\gamma_{sm}\phi}{k''(1-\phi)} \qquad (15)$$

We can accordingly rewrite the C-term in the approximate form (taking $\phi = 0.5$) as –

$$Cu = \frac{1}{30}\left(\frac{k''}{1+k''}\right)^2 \frac{d_p^2 u}{D_{sm}} \qquad (16)$$

Where $D_{sm} = \gamma_{sm} D_m$ is the diffusion coefficient for the solute in the stagnant mobile phase with the particles. The maximum C-value is obtained with large k''. If we take $u = 1\,mm\,s^{-1}$, $D_{sm} = 0.6 \times 10^{-9}\,m^2\,s^{-1}$ we obtain

$$Cu = 55 \times (d_p/mm)^2 = 55 \times 10^{-6}(d_p/\mu m)^2 \qquad (17)$$

and with $d_p = 5\mu m$ $Cu = 1.3\mu m$
with $d_p = 0.5\mu m$ $Cu = 0.13\mu m$

It is thus clear that if CEC can be achieved with sub-micron particles both the A-term and C-term contributions to H should become insignificant compared to the contribution to axial diffusion. Thus eq. (10) applies again.

We conclude that the ultimate limitation to performance in all Capillary Electroseparation methods is axial diffusion. Thus we reach the following equations for ultimate performance:

Ultimate Plate Height $\quad H = \dfrac{2D_m\eta}{\epsilon_0\epsilon_r\zeta E}$: $\quad H \alpha 1/E$

Ultimate Plate Number $\quad N = \dfrac{L}{H}\dfrac{\epsilon_0\epsilon_r\zeta V}{2D_m\eta}$: $\quad N \alpha V$

Ultimate dead time $\quad t_0 = \dfrac{L}{u} = \dfrac{L^2\eta}{\epsilon_0\epsilon_r\zeta V}$ $\quad t_0 \alpha L^2$; $\quad t_0 \alpha (1/V)$

In order to obtain high plate counts we require high voltages ($N \alpha V$). In order to obtain rapid elution we require both high voltages ($t_0 \alpha 1/V$) and short columns ($t_0 \alpha L^2$). If voltage is increased and column length decreased then the potential gradient E and consequent heat release per

unit volume of electrolyte will increase. The ultimate limitation on performance will thus be determined by how well these adverse thermal effects can be controlled. Similar conclusions have been reached by Jorgenson for CZE [1, 5].

Heat Release and Temperature Excess

When a current is passed along a cylindrical conductor ohmic heat is released and the conductor heats up. Fig. 4 indicates diagramatically the temperature distribution for an insulated conductor such as the capillary in a CES system. Over the central region heat is generated homogeneously and the temperature variation across the bore of a cylindrical tube (i.e. conductor) is parabolic. The heat so generated is conducted first through the walls of the tube and then through the surrounding air. Because of the magnitudes of the relevant thermal conductivities, typical values of which are given in Table III, the thermal gradient is largest in the air zone and least in the tube wall. The heat release per unit volume in an electrolyte is given by

$$Q = E^2 \lambda c \epsilon \qquad (18)$$

where λ is the molar conductivity of the solution, c its concentration and ϵ the total porosity of the medium: ϵ will be unity for an open tube and from 0.4 to 0.8 for a packed tube. With typical values $E = 50{,}000\,V\,m^{-1}$, $\lambda = 0.015\,m^2\,mol^{-1}\,\Omega^{-1}$, $C = 10\,mol\,m^{-3}$, $\epsilon = 0.80$ we obtain $Q = 300 \times 10^6\,W\,m^{-3} = 300\,W\,cm^{-3}$.

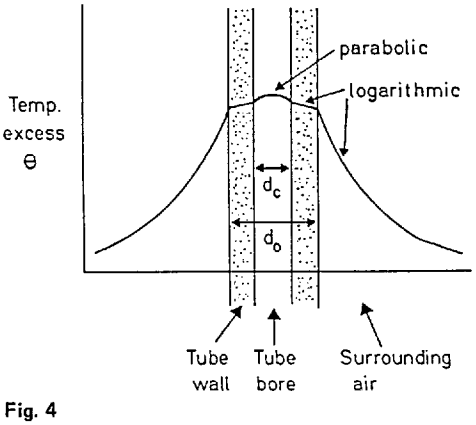

Fig. 4

Semi-quantitative representation of temperature profile across a tube containing electrolyte heated by passage of an electric current.

Table III. Typical thermal conductivities, κ.

Air	$0.025\,W\,m^{-1}\,K^{-1}$
Water	$0.6\,W\,m^{-1}\,K^{-1}$
Methanol	$0.2\,W\,m^{-1}\,K^{-1}$
Quartz	$1.4\,W\,m^{-1}\,K^{-1}$
Borosilicate Glass	$1.0\,W\,m^{-1}\,K^{-1}$

The temperature excess, θ_{core}, within the core region (i.e. the difference between the temperature on the axis of the tube and at its inner wall) is given by

$$\theta_{core} = Qd_c^2/16\kappa = (E^2 \lambda c \epsilon)(d_c^2/16\kappa) \qquad (19)$$

For $d_c = 100\mu m$ and $\kappa = 0.4\,W\,m^{-1}\,K^{-1}$, $\theta_{core} = 0.47\,K$

The temperature excess across the wall, θ_{wall}, is given by

$$\theta_{wall} = \frac{Qd_c^2}{8\kappa_w} \ln\left(\frac{d_0}{d_c}\right) \qquad (20)$$

where d_0 is the outer diameter of the tube and κ_w is the thermal conductivity of the tube wall. Again using typical values $d_0/d_c = 2.0$ and $\kappa_w = 1.0\,W\,m^{-1}\,K^{-1}$ we obtain $\theta_{wall} = 0.11\,K$. Thus both θ_{core} and θ_{wall} are small. The temperature excess of the tube wall relative to the surrounding ambient air is much larger as is now shown.

Heat generated in a (horizontal) tube in air is lost mainly by natural convection or by forced convection rather than by simple conduction through still air. In the case of natural convection it can be shown by dimensional analysis [21] that a universal plot of $\log(Qd_c^2/\theta\kappa)$ against $\log(\theta d_c^3/\mu^2)$ can be constructed where μ is the kinematic viscosity of air (i.e. viscosity/density). Similarly for forced convection a universal plot of $\log(Qd_c^2/\theta\kappa)$ against $\log(ud_c/\mu)$ can be constructed. The appropriate plots drawn after Roberts [21] are shown in Fig. 5.

To obtain the temperature rise θ for natural convection, lines such as the dotted line in Fig. 4, are drawn for specific values of (Qd_c/κ) and (d_c^3/μ^2) for a range of θ-values. The intersection of the dotted line with the full line (marked by a filled point) gives the appropriate value of θ. In the case of forced convection, the value of (ud_c/μ) is first evaluated and then the value of θ readily found knowing (Qd_c^2/κ).

Fig. 6 shows plots for natural convection giving the temperature excess θ for various tube diameters and Q values. In this case the Q-values are to be taken as those based upon the outside diameter of the tube. This can formally be accommodated by adjusting ϵ in eq. (18) when working

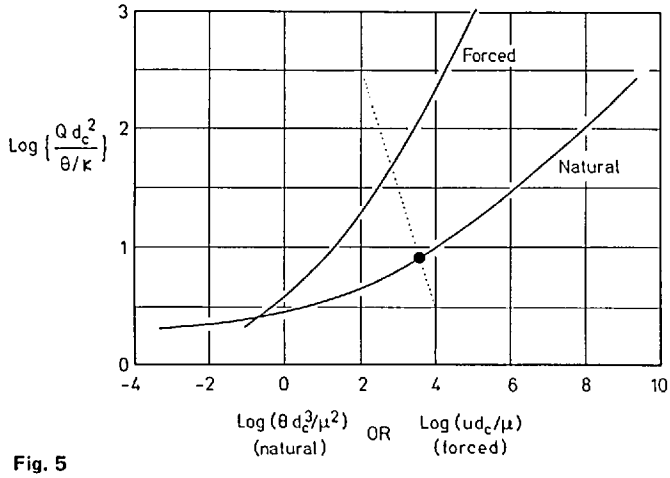

Fig. 5

Characteristic plots for natural and forced convection – after Roberts [21]. For explanation of dotted line see text. For explanation of symbols see text and glossary.

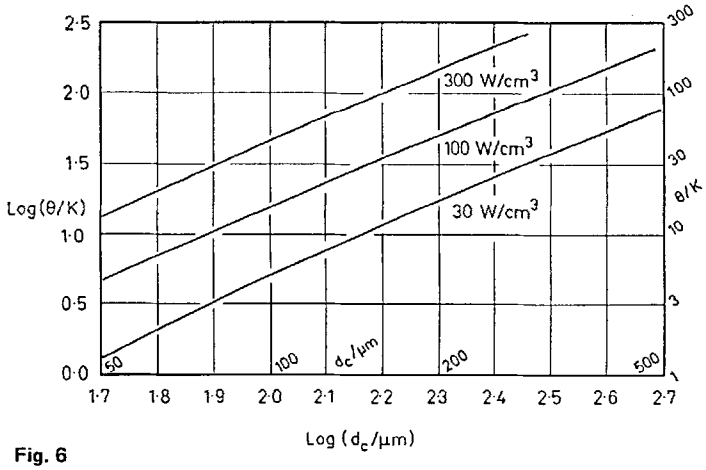

Fig. 6

Dependence of temperature rise, θ, upon tube diameter, d_c, for various rates of heat output in a homogeneously heated cylinder (or tube) with natural convection.

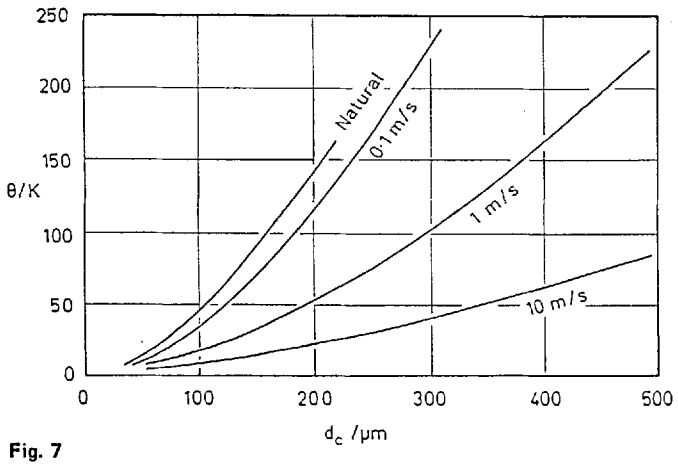

Fig. 7

Temperature rise, θ, for different tube diameters under natural and forced convection (air velocity given on curves) for a heat output of 300 W cm^{-3}.

out Q. With power outputs of 300 W cm^{-3} a temperature difference of 50 K will occur between a tube with a diameter of about 100 μm and the surrounding air. The temperature excess within the tube itself will be only a matter of one degree. If the power output is 30 W cm^{-3} then a tube up to 350 μm bore can be used before a temperature excess of 50 K is attained.

Although the lines in Fig. 6 are not straight they are nearly so and over the ranges shown are quite well approximated by eq. (21)

$$\text{Log}\,(\theta/\text{K}) = 1.70 \log (d_c/\mu\text{m}) + \log (Q/\text{W cm}^{-3}) - 4.20 \qquad (21)$$

Temperature excesses of the order of several tens of degrees are well known in CES systems and have been noted by several workers. They are responsible for the curvature of plots of electroendosmotic velocity, u_{eo}, against applied voltage or field gradient [22]. Thus, for example, a temperature rise from 20°C to 70°C will cause the viscosity of water to fall from 1.00×10^{-3} to 0.61×10^{-3} kg m^{-1} s^{-1} and so, according to eq. (2), will cause u_{eo} to increase by a factor of 1.64.

Evidently the conditions under which CES techniques can be carried out, using only natural convective cooling, are quite restricted, especially when there is a trend towards using higher field strengths in order to obtain faster analysis.

The use of forced convection is therefore highly desirable although there will be difficulties in adequately cooling those parts of tubes which pass through detectors and other pieces of equipment. The effects of natural and forced convection are compared for a specific power output (300 W cm^{-3}) in Fig. 7. Forced convection velocity of 10 m s^{-1} will reduce the temperature excess about fivefold compared to natural convection. Fig. 7 can be used to determine θ values for other power outputs by noting, from Fig. 5, that the temperature excess for any value of the air velocity is proportional to $Q d_c^2$. Thus referring again to Fig. 7, if the power output were 33 W cm^{-3} instead of 300 W cm^{-3} the numerical values on the d_c-axis would be increased 3 times.

It is concluded that forced air cooling of the capillary tube in all CES systems is desirable with a flow velocity of at least 10 m s^{-1}. It will be particularly important as we move to higher E-values to ensure that all parts of tubes are adequately cooled, in particular those sections that pass through other pieces of equipment such as detectors, injection systems etc.

Peak Dispersion arising from Self Heating

The temperature difference between the tube in CES relative to the surrounding air does not, in itself, affect the plate height or plate count, but the variation of temperature within the electrolyte does. The plate height contribution from this can be quite significant and can seriously reduce the efficiency of a CES separation.

The parabolic temperature profile which exists across the capillary tube may cause variations in migration rates due to one or more of three possible effects —

(a) Changes in electrolyte viscosity, η.
(b) Changes in partition ratios between phases k'.
(c) Changes in the rates of kinetic processes.

Taking viscosity as typical, its variation over a small temperature range, say up to 10 K, can be written as —

$$d\eta/\eta = \alpha_v \theta \qquad (22)$$

where $\alpha_v = 0.026$ for water and 0.013 for methanol.

Similarly for partitioning between phases

$$dk'/k' = \alpha_{k'} \theta \qquad (23)$$

In general the activation energy for viscosity is about half the heat of volatilization of a liquid, but in typical liquid partition systems the heat of transfer between phases is much less than this. Thus, in general, $\alpha_{k'} \ll \alpha_v$.

Kinetic effects should be important in CGE where diffusion is obstructed by the strands of the polymer gel.

Table IV. Estimated proportional change in physical parameters with temperature, α.

Method	Proportional variation in u per Kelvin due to variation of				
	Viscosity as it affects		Partition Coefficient	Rate of Kinetic Processes	Total
	Flow rate	Migration rate			
CZE	–	0.02	–	–	0.02
CGE	–	0.02	–	0.02	0.04
CMEC	–	0.02	0.01	–	0.03
CEC	0.02	–	0.01	–	0.03

Here we are dealing with an effect analogous to viscosity and the appropriate α-value could be similar to that for viscosity.

Variations in the properties (a) to (c) may or may not affect migration rates. For example in CZE the electroendosmotic velocity is not affected by the temperature variation since shearing arises only in the region very close to the wall (e.g. within 0.1 μm). On the other hand the electrophoretic velocities of ions will vary across the tube since they depend upon the local viscosity of the electrolyte.

Table IV summarises how changes in the three properties might be expected to affect the migration rate. In general

$$\delta u_{mig}/u_{mig} = \theta_{core} \Sigma \alpha_i = \alpha\theta_{core} \quad (24)$$

where the summation of the α_i is over all relevant effects. For typical calculation we take the overall total α-value as 0.03.

The parabolic temperature variation across the tube results in a parabolic variation of velocity which will be superimposed on a main migration velocity of the band as a whole. The situation is compared to that of viscous (pressure-driven) flow in an open tube in Fig. 8. The full lines for both cases show the positions of elements of fluid after times t_1, t_2 and t_3 where all elements start initially at the position marked zero.

The case of viscous flow was treated by Taylor and Aris [23, 24].

The parabolic flow profile tends to cause dispersion of any band of solute which starts at a given cross section in the tube (e.g. that marked zero in Fig. 8). This dispersive tendency is counteracted by transverse diffusion. The interaction of the two effects produces a band of solute with a Gaussian concentration profile (measured along the axis of the tube) whose variance, in units of length, is given by

$$\sigma_z^2 = \frac{L d_c^2 \bar{u}}{96 D_m} \quad (25)$$

where $\bar{u}$ is the mean flow velocity, equal to half of the linear velocity at the axis of the tube.

The plate height for an unretained solute in chromatography is then –

$$H = \frac{\sigma_z^2}{L} = \frac{d_c^2 \bar{u}}{96 D_m} \quad (26)$$

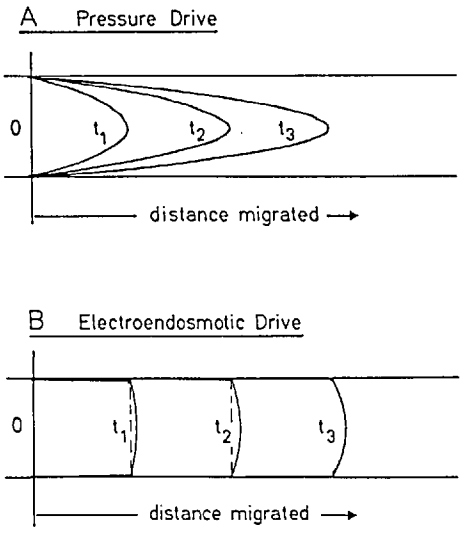

Fig. 8

Parabolic displacement profiles in open tubes in the absence of lateral diffusion after times t_1, t_2 and t_3 (A) with pressure driven flow, (B) with electroendosmotic flow where self heating causes variation of migration rate. Mean flow rate in B is approximately twice that in A.

In the case of CES systems with self heating of the liquid core, we experience a small parabolic disturbance superimposed on the uniform migration velocity of solute along the tube. The mean velocity $\bar{u}$ of the Taylor-Aris equation is thus replaced by the mean excess velocity $\delta\bar{u} = \frac{1}{2}\delta u_{mig}$ where δu_{mig} is the difference between the velocity at the axis and at the wall and given by eq. (24). The effective distance of migration of the disturbance becomes $(\delta\bar{u}/u_{mig})L$. Making these substitutions in eq. (25) gives

$$\sigma_z^2 = \frac{(\delta\bar{u}/u) L \times d_c^2 \times \delta\bar{u}}{96 D_m} = \frac{(\delta\bar{u}/u)^2 L d_c^2}{96 D_m} u \quad (27)$$

We then substitute for $(\delta\bar{u}/u)$

$$\delta\bar{u}/u = \tfrac{1}{2}(\delta u_{mig}/u_{mig}) = 0.015\theta_{core} \quad (28)$$

to give

$$H = \frac{\sigma_z^2}{L} = \frac{(0.015\theta_{core})^2 d_c^2 u_{mig}}{96 D_m} \quad (29)$$

Finally we substitute for θ_{core} from eq. (19) and use the electroendosmotic velocity for u_{mig} to give the thermal contribution to the plate height, H_{TH}, as

$$H_{TH} = 10^{-8} \frac{\epsilon_0 \epsilon_r \delta}{D_m \eta \kappa^2} E^5 d_c^6 \lambda^2 c^2 \quad (30)$$

With typical values of the constants, $E = 50{,}000\ V\ m^{-1}$ and $C = 10\ mol\ m^{-3}$ we obtain

$H_{TH} = 0.006\mu m$ with $d_c = 100\mu m$

$H_{TH} = 0.4\mu m$ with $d_c = 200\mu m$

Thus H_{TH} is generally insignificant for narrow bore columns but can quickly become dominant (compared to

$H = 1.1\mu m$ arising from axial diffusion) if either E, d_c or c are allowed to rise beyond a certain limit.

We are not, however, particularly interested in H_{TH}, per se, but rather in how it compares to H_{CES}, the ultimate value of H in CES arising from axial diffusion. We therefore examine the effect of imposing the condition

$$H_{CES} > 10\,H_{TH} \tag{31}$$

Using eq. (11) for H_{CES} and eq. (30) for H_{TH} we obtain

$$\frac{2D_m u}{\epsilon_0 \epsilon_r \zeta E} > 10 \times 10^{-8} \frac{\epsilon_0 \epsilon_r \zeta}{D_m \eta \kappa^2} E^5 d_c^6 \lambda^2 c^2 \tag{32}$$

or

$$d_c^3 E^3 c > 4500 \frac{D_m \eta \kappa}{\lambda \epsilon_0 \epsilon_r \zeta} \tag{33}$$

Using typical values for parameters on the righthand side of eq. (33) gives

$$\left\{\frac{d_c}{\mu m}\right\}^3 \left\{\frac{E}{kV\,m^{-1}}\right\}^3 \left\{\frac{c}{mol\,dm^{-3}}\right\} < 3.3 \times 10^9 \tag{34}$$

Table V shows the effect of the restriction (34) on the column bores which can be used under various operating conditions.

Table V also lists the power generation rate Q for each case and the excess temperature between the tube and the surrounding air if the tube is cooled by an air flow at $10\,m\,s^{-1}$.

Allowed tube bores range from 1500 to $30\mu m$ as the operating conditions change from $E = 10\,kV\,m^{-1}$, c = 0,001M to $E = 100\,kV\,m^{-1}$, c = 0.1M while the temperature rises change from 1 to 50K.

Table V shows that while current tube bores of around $100\mu m$ with E values of $50\,kV\,m^{-1}$ are well below the limit at which thermal dispersion becomes important, it will certainly be necessary to go to narrower tubes if higher fields and/or electrolyte concentrations become desirable.

Preparative Possibilities of SEC Methods

The possibility of using tubes as wide as 1.5mm (see Table V top left hand entry) raises the attractive possibility of preparative separations. Such a conclusion could, however, be illusory. Broadly speaking, the maximum solute concentrations which can be applied without band distortion will be proportional to the electrolyte concentrations. Thus going down the column headed $10\,kV\,m^{-1}$ the solute concentration could be increased 100-fold while the tube area decreases 22 times. Accordingly the throughput would be greatest for the $320\mu m$ tube containing 0.1M electrolyte. Going across the table the elution velocity would increase 100 fold from 10 to $100\,kV\,m^{-1}$, but the tube area would decrease 100-fold, so there would be no loss or gain from changing the potential gradient. We therefore conclude that maximum throughput will be achieved with a high electrolyte concentration and a tube which is sufficiently narrow to avoid deterious heat effects. Since there is no advantage in going to high fields strengths, a moderate field is recommended as more convenient and requiring less highly tuned equipment.

Table V. Boundary conditions under which plate height contribution from thermal effects is less than 0.1 times plate height contribution from axial diffusion.

C/mol dm^{-3}	E/kV m^{-1}	10	20	50	100	
		1500	750	300	150	d
	0.001	1	5	30	120	Q
		2	3	4	6	θ
		700	350	140	70	d
	0.01	12	50	300	1200	Q
		6	8	15	19	θ
		320	160	60	30	d
	0.1	120	500	3000	12000	Q
		20	26	40	50	θ

d = Maximum allowed tube diameters, in μm

Q = Heat production rate, in $W\,cm^{-3}$

θ = Temperature difference in Kelvin between tube wall and surrounding air, with air flow at $10\,m\,s^{-1}$

References

[1] *J. W. Jorgenson, K. D. Lukacs*, J.H.R.C.C.C., **4**, 230–231 (1981).

[2] *J. S. Green, J. W. Jorgenson*, J.H.R.C.C.C., **7**, 529–531 (1984).

[3] *H. H. Lauer, D. McManigill*, Analyt Chem., **58**, 166–170 (1986).

[4] *T. Tsuda, K. Nomura, G. Nakagawa*, J. Chromatogr., **264**, 385–392 (1983).

[5] *J. W. Jorgenson*, A.C.S. Symposium Ser., **335**, 182–198 (1987).

[6] *A. S. Cohen, D. Najarian, J. A. Smith, B. L. Karger*, J. Chromatogr., in press 1988.

[7] *A. S. Cohen, B. L. Karger*, J. Chromatogr., **397**, 409–417 (1987).

[8] *A. S. Cohen, D. Najarian, A. Paulus, A. Gultman, J. A. Smith, B. L. Karger*, Proc. Nat. Acad. Sci. (New York), in press 1988.

[9] *S. Terabe, K. Otsuka, K. Ichikawa, A. Tsuchiya, T. Ando*, Analyt. Chem., **56**, 111–113 (1984).

[10] *S. Terabe, K. Otsuka, T. Ando*, Analyt. Chem., **57**, 834–841 (1985).

[11] *S. Terabe*, in press 1988.

[12] *A. S. Cohen, S. Terabe, J. A. Smith, B. L. Karger*, Analyt. Chem., **59**, 1021–1027 (1987).

[13] *A. T. Balchunas, M. J. Sepaniak*, Analyt. Chem., **59**, 1466–1470 (1987).

[14] *V. Pretorius, B. J. Hopkins, J. D. Schieke*, J. Chromatogr., **99**, 23–30 (1974).

[15] *J. W. Jorgenson, K. D. Lukacs*, J. Chromatogr., **218**, 209–216 (1981).

[16] *J. H. Knox, I. W. Grant*, 16th Int. Symp. on Column Liquid Chromatography, Washington, U.S.A., 19–24 June 1988, Abstract No. M-L-5.

[17] *J. O'M. Bockris, B. W. Conway, E. Yeager*, Ed., "Comprehensive Treatise of Electrochemistry", Plenum Press, New York, London, Vol. 1, pp. 404–414.

[18] *J. H. Knox, H. P. Scott*, J. Chromatogr., **316**, 311–332 (1984).

[19] *C. L. Rice, R. Whitehead*, J. Phys. Chem., **69**, 4017–4024 (1965).

[20] *J. H. Knox, I. W. Grant*, Chromatographia, **24**, 135–143 (1987).

[21] *J. K. Roberts*, "Heat and Thermodynamics", 3rd Edn. Blackie, London, 1947, pp 245–251.

[22] *K. D. Altria, C. F. Simpson*, Anal. Proc. R.S.C., **23**, 453–454 (1986).

[23] *Sir G. I. Taylor*, Proc. Roy. Soc. (London), **A219**, 186 (1953).

[24] *R. Aris*, Proc. Roy. Soc. (London), **A235**, 67 (1953).

Received: Dec. 29, 1988
Accepted: Jan. 17, 1989
G

Glossary of Symbols

(underlined values are constants)

		Value of constant* or typical value of property
A, B, C	Constants in Van Deemter equation	
c	Concentration of electrolyte	10^{-2} mol dm^{-3}
d_c	Column Bore	100 μm
D_m	Diffusion coefficient of solute in free solution	1.0×10^{-9} m^{2}s^{-1}
d_0	Column outside diameter	200 μm
d_p	Particle diameter	
D_s	Diffusion coefficient in stationary phase	$\ll$ Dm
D_{sm}	Diffusion coefficient in stagnant mobile phase	$\cong$ Dm
D_{sz}	Diffusion coefficient in stationary zone	$\cong$ Dm/k''
E	Electrical Potential Gradient = V/L	50 kV m^{-1}
F	Faraday constant	<u>96500 C mol^{-1}</u>
H	Plate Height	
H_{CES}	Plate Height contribution from CES processes	
H_{TH}	Plate Height contribution from thermal effects	
k'	Phase capacity ratio	
k''	Zone capacity ratio	
L	Column Length	0.5 m
Q	Heat output per unit volume (power density)	300 W cm^{-3}
R	Gas constant	<u>8.314 JK^{-1}mol^{-1}</u>
t_0	Dead time in column	
T	Temperature	300 K
u	Migration velocity	1 mm s^{-1}
$\bar{u}$	Mean velocity	
u_{mic}	Electrophoretic velocity of micelles	
u_{eo}	Electroendosmotic velocity	1 mm s^{-1}
u_{ep}	Electrophoretic velocity	
u_{oep}	Velocity in obstructed electrophoresis (CGE)	
u_x	Migration velocity of solute X	
V	Voltage applied across column	25 kV

		Value of constant or typical value of property
α, α_i	Fractional change per Kelvin in a property	0.03 K^{-1}
α_v	Fractional change per Kelvin in viscosity	
$\alpha_{k'}$	Fractional change per Kelvin in capacity ratio	
γ	Obstructive factor for diffusion	
γ_s	Obstruction factor for diffusion stationary phase (CEC)	
γ_{sm}	Obstructive factor for diffusion in stagnant mobile phase	
δ	"Thickness" of electrical double layer	3 nm
ϵ	Bed porosity for CEC	0.8
ϵ_0	Permitivity of vacuum	<u>8.85×10^{-12} C^2 N^{-1} m^{-2}</u>
ϵ_r	Relative permitivity or dielectric constant	80
η	Viscosity	0.001 kg m^{-1} s^{-1}
κ	Thermal conductivity	see Table III
κ_w	Thermal conductivity of wall of tube	see Table III
λ	Molar conductivity; tortuosity factor in Van Deemter equation	0.015 m^2 mol^{-1} Ω^{-1}
μ	Kinematic viscosity	
μ_{ep}	Electrophoretic mobility	
ϕ	Fraction of eluent which is stagnant in CEC	0.5
σ_z^2	Variance of peak in length units	
θ	Temperature difference across any region especially between wall of tube and surrounding air	50 K
θ_{core}	Temperature difference between axis and inner wall of tube	0.5 K
θ_{wall}	Temperature difference across wall of tube	0.1 K
χ	Obstructive factor in capillary gel electrophoresis	
ζ	Zeta potential	50 mV

* Values of constants underlined